Dyes and Pigments 94 (2012) 427–436

Contents lists available at SciVerse ScienceDirect

Dyes and Pigments

journal homepage: www.elsevier.com/locate/dyepig

Rhodamine solid complexes as fluorescence probes to monitor the dispersion of cyclodextrins in polymeric nanocomposites

R. Serra-Gómez [a], G. Tardajos [b], J. González-Benito [c], G. González-Gaitano [a,*]

[a] Dpto de Química y Edafología, Universidad de Navarra, Facultad de Ciencias, 31080 Pamplona, Navarra, Spain
[b] Dpto. Química-Física I, Universidad Complutense de Madrid, Spain
[c] Dpto. C. Ing. Materiales Ing. Química, Universidad Carlos III de Madrid, Spain

ARTICLE INFO

Article history:
Received 23 November 2011
Received in revised form
8 February 2012
Accepted 10 February 2012
Available online 22 February 2012

Keywords:
Cyclodextrins
Rhodamine
Polymeric nanocomposite
High energy ball milling
Fluorescence probe
NMR

ABSTRACT

Rhodamines B and 6G have been used to evaluate the dispersion of β-Cyclodextrin in a thermoplastic matrix, poly(ethylene-co-vinyl acetate), by high energy ball milling. In a first stage, a study of the binding properties of β-Cyclodextrin with both fluorophores has been carried out, to determine which of them forms the most stable complex with the macrocycle, its topology and to check whether their fluorescence is kept after the milling process. Both systems have been fully characterized in the solid state (FTIR and XRD, TGA and fluorescence spectroscopy), and in solution (^{1}H NMR ROESY, steady state and time-resolved fluorescence spectroscopy). Then, nanocomposites based on the thermoplastic matrix and the cyclodextrin complexes have been cryomilled and processed in the form of thin films. Only Rhodamine B forms a complex stable enough to track the nanofiller dispersion within the polymer. This labeled cyclodextrin is uniformly dispersed throughout the matrix after the milling and film forming, yielding a blue-shifted and remarkably enhanced fluorescent response when compared to the same material prepared with the mixture of Rhodamine B and β-Cyclodextrin.

1. Introduction

Polymer nanocomposites are generally built by homogeneous dispersion of a nanoscopic filler (nanofiller) into the polymeric matrix [1]. Because of the large surface to volume ratio of nanoparticles, the interphase formed between the nanoparticles and the polymer constitutes a greater fraction of the whole material than in common composites, even with small amounts of the nanofiller (less than 5% by weight), a feature which has important consequences on the final properties of the material [2]. Obtaining a perfectly homogeneous dispersion is critical for a nanocomposite to have the properties that are expected. However, regardless of the method used for the mixing, this issue becomes more critical the smaller the nanofiller is. Recently, high energy ball milling (HEBM), a conventional method used for synthesis and processing of inorganic materials [3–5], has been revealed as a new way of processing thermoplastic matrix nanocomposite materials, not only due to its potential results in terms of nanoparticle dispersion, but also from an economical and clean point of view. Although the mechanical action may have adverse effects of wearing on solid polymers by mechanisms of chain scission and sample oxidation, HEBM has been successfully used to obtain polymer blends with improved mechanical properties and polymer nanocomposites with a real dispersion of nanoparticles [6–10].

Cyclodextrins (CDs) are cyclic oligosaccharides composed of 6, 7 or 8 D-glucopyranose rings termed α, β and γCD respectively. Their sizes (ca. 1 nm) fall within the lower limit of the nanometric scale so they can be considered as a limiting type of nanofiller. CDs are shaped like truncated cones, with a hydrophobic cavity and a hydrophilic exterior. The precise number of hydroxyl groups according to the number of glucose units makes it possible to establish strong interactions with certain polymeric matrices. CDs can also be easily modified with other functional groups which allow modulating such interactions according to the nature of the matrix, or can be grafted to common nanofillers (nanoparticles, layers,…) for improving the properties of the material. The ability to form inclusion complexes with organic molecules inside the cavity, e.g. a monomer for its further polymerization [11] also represents an added value to produce a material with features different from those of the single constituents of the nanocomposite. Yet, in spite of their exclusive properties the use of CDs in the field of nanocomposites is still very limited [12–14].

* Corresponding author. Tel.: +34 948 425 600x6315.
E-mail address: gaitano@unav.es (G. González-Gaitano).

0143-7208/$ – see front matter © 2012 Elsevier Ltd. All rights reserved.
doi:10.1016/j.dyepig.2012.02.009

A problem that arises when dispersing CDs in a polymer comes from the reduced size of these macrocycles, which makes it difficult to confirm that an adequate dispersion has taken place. AFM, SEM or TEM microscopy can be used to this purpose, but these are techniques which involve sample preparation processes that require a consistent amount of time and effort, more focused to a final product characterization and not convenient for regular checks. In addition to that, the electron beam can melt the matrix when thermoplastic polymers are being used.

A different approach may be to use fluorescence microscopy by previously tagging the CD by inclusion of a fluorophore in the cavity, provided it is stable enough. Rhodamine-based dyes present unique fluorescent properties and are therefore used in a wide variety of applications, ranging from applied chemistry and physics to biochemistry or microbiology [8]. Rhodamines are known to interact with βCD in different ways, depending on the state of aggregation of the fluorophore and its molecular form [15,16], increasing or decreasing the fluorescence quantum yield as a result of their interaction. In the solid state, however, the number of investigations is limited, most of them related to the development of solid state dye lasers [17,18] or to the use of CD-based resins to adsorb organic dyes [19].

In this work we propose the use of the fluorescent properties of Rhodamine B and Rhodamine 6G (hereafter RhB and Rh6G, Fig. 1a and b) and their ability to form complexes with βCD (Fig. 1c), to produce a solid complex that acts as a fluorescent probe to evaluate the dispersion of these oligosaccharides into a thin-film polymeric nanocomposite material prepared by HEBM. The polymeric matrix used here is ethylene vinyl acetate (EVA), a thermoplastic polymer with polar vinyl acetate groups and crystalline ethylene domains. EVA copolymers are a good choice to combine with these fluorophores, as they present optical homogeneity and organic dyes usually show good compatibility with polymeric matrices. In addition, their easy processability makes them excellent for miniaturization and to be included in other composite systems [20].

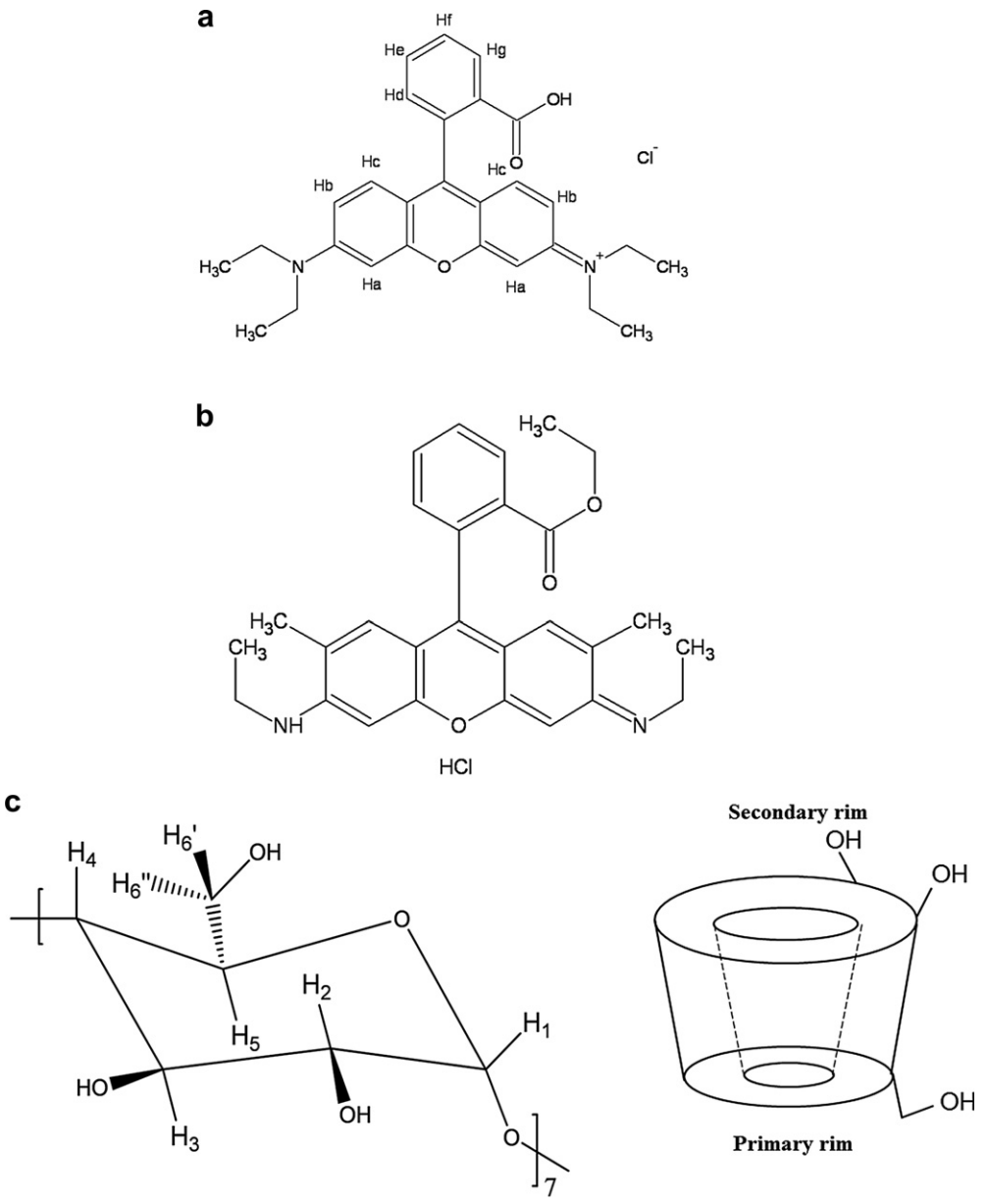

Fig. 1. (a) Rhodamine B; (b) Rhodamine 6G; (c) Scheme of β-Cyclodextrin.

In this research we have focused on the dispersion of the macrocycle as the nanofiller in the polymer, leaving the grafting of the βCD to nanoparticles and further nanocomposite synthesis for future projects. The first step is to evaluate that the complexes between the fluorophore and the CD form and are stable enough to endure the HEBM process, that they present a different fluorescent response when attached to the βCD than in free form and that they can be dispersed homogenously, so they can be used as dispersion fluorescence probes in nanomaterials. For this purpose the systems have been previously studied in solution to characterize their complex formation characteristics (stability, temperature dependence, stoichiometry and topology) and the fluorescent emission. Finally, the solid state products are tested and combined with the polymer using the HEBM method, to verify their adequate dispersion and whether their properties are retained along the nanocomposite processing.

2. Materials and methods

2.1. Materials

Rhodamine B 99% pure (Basic Violet 10; C.I. 45170; 9-(2-Carboxyphenyl)-3,6-bis(diethylamino)xanthylium chloride) and Rhodamine 6G 99% pure (Basic Red 1, C.I. 45160, ethyl 2-(6-(ethylamino)-3-(ethylimino)-2,7-dimethyl-3H-xanthen-9-yl)benzoate monohydrochloride) were purchased from Acros Organics. β-Cyclodextrin was bought from Wacker Chemicals (Cavamax Pharma, 99.5% pure). Polyethylene-co-vinyl acetate (composition 12% by weight in vinyl acetate, density 0.933 g/cm^3 at 25 °C, Vicat temperature ASTM D 1525 = 65 °C and melting point 95 °C), was supplied by Sigma Aldrich.

2.2. Sample preparation

RhB:βCD complex was prepared by mixing a RhB 2.5×10^{-3} M aqueous solution with βCD at an equimolar ratio followed by stirring for 10 min, poured into a crystallizer and placed in the stove at 70 °C until solvent evaporation. The resulting solid is a dark red flaked product. The physical mixture of RhB and βCD was prepared by weighing the same amounts used for the complex preparation and mixing them in a vortex shaker, resulting in a greenish powder mixture. The same procedure was carried out with Rh6G. In this case the solid mixture and the compound prepared by crystallization did not show any visual differences.

A mixture of 5% by weight of RhB:βCD and EVA was subjected to HEBM under cryogenic conditions (cryomilling) in a MM400 RETSCH miller. Stainless steel milling tools (a vessel of 50 mL of capacity and one ball of 20 mm diameter) were used. The process was carried according to the following protocol: 1 h of active cryomilling divided into 12 cycles of 5 min of milling at 25 Hz and 15 min of resting in liquid nitrogen. Another vessel endured the same procedure with the physical mixture of RhB and βCD and the EVA at the same proportions (95% by weight of EVA).

Thin films were prepared by hot pressing. The powder obtained from the milling processes was deposited between two Teflon plates and then pressed and heated in an oven at 150 °C for 20 min. After that, the prefilms obtained were cooled inside the oven down to 40 °C. A small portion of the prefilm (about 9 mm^2) was then sandwiched between the two Teflon plates and clamped within two stainless steel plates, introduced in a preheated oven at 150 °C and heated for 120 min. The film was slowly cooled down inside the oven to room temperature, thus avoiding any thermal stress in the sample.

2.3. Characterization techniques

The crystalline structure of materials under study was characterized by X-ray diffraction, XRD, on randomly oriented powder preparations using a Bruker D8 Advance diffractometer with a X Kristalloflex K760 X-Rays generator, with a copper anode emitting typical X radiation $K_{\alpha 1} = 1.5417$ Å at 40 kV and 30 mA. Diffraction angles were monitored from $2\theta = 2°–40°$ at a rate of 3 s/step (0.02° in 2θ). Analysis of the XRD patterns was carried out with XRD Wizard 2.4.11 software (Bruker GmbH). FTIR-ATR analyses of powder and films were performed with a FTIR-ATR Nicolette Avatar 360, using a resolution of 2 cm^{-1} and averaging 32 scans. Spectral analysis treatment was undertaken with the OMNIC E.S.P. v5.1 software (Nicolet). Thermogravimetric analysis, TGA, was carried out in a TGA-SDTA 851 Mettler Toledo. Samples were subjected to a heating program from 25 °C to 600 °C at a heating rate of 10 °C/min under a N_2 atmosphere.

Fluorescence studies were undertaken using an Edinburgh Instruments FLS920 spectrofluorimeter equipped with a 450 W Xenon arc lamp. Samples were excited at 553 nm and the emission recorded from 560 to 750 nm under constant stirring, averaging 5 scans with a 1 nm step and 0.1 s dwell time. Excitation and emission slits were 2 nm and 3 nm, respectively. Measurements in solution were carried out at 15 °C, 25 °C, 35 °C and 45 °C in a 10 mm path length quartz cuvettes controlled by a Lauda Ecoline RE104 thermostat. Each isotherm was repeated three times. For the solid samples the powder or a portion of the film was sandwiched between two quartz glasses in the instrument sample holder. Fluorescence lifetimes were measured with the same equipment using as the radiation source a PDL800-B Picoquant pulse diode driver and 455 nm and 500 nm diodes, with full width at half maximum (FWHM) of 1600 and 1700 ps, respectively. The instrument response was measured by using a Ludox 30% aqueous suspension, purchased from Aldrich. Data treatment was performed with FAST v3.0 software (Edinburgh Instruments). The films were observed with an Olympus CH40 fluorescence microscope equipped with a ColorView camera (Soft Imaging Systems).

NMR experiments were performed in a Bruker Avance 700 Ultrashield (700 MHz). The samples were prepared in D_2O (99.990% in deuterium purchased from Sigma Aldrich), with no buffers added, using the HDO signal as the reference. Monodimensional experiments were done by averaging 256 scans. ROESY experiments were carried out on 32 scans with presaturation of the solvent signal [21] by using the pulse sequence described in the literature [22], with an optimal mixing time of 600 ms. Temperature was set to 25 °C in all cases.

3. Results and discussion

3.1. Complexes in solution: stoichiometry, stability and structure

As a first stage, the complexes between rhodamines and βCD have been investigated. The analysis of the chemical shifts of the ^{1}H NMR signals of the complex in relation to the signals from the pure RhB and βCD (Table 1 and Figs. 2 and 3) are the main indication of the extent of the complex formation. For the βCD, the protons undergoing the most important changes are the H_6 and H_5, i.e., those located at the mid-bottom inner side of the cavity and at the narrower rim of the macrocycle, respectively. Less significant changes were noted for the inner H_3, at the mid-upper part of the CD. Finally, tiny shifts are detected in the outer protons H_1, H_2 and H_4. All these resonances except that for H_4 shift upfield. If we consider now the guest molecule, RhB, the protons of the substituents CH_3– and CH_2– (downfield) and the H_D (upfield) experience

Table 1
Changes in the chemical shifts of protons of βCD and RhB.

H	Free δ (ppm)	$\Delta\delta$ (ppm)
β-Cyclodextrin		
H_1	4.949	0.039
H_2	3.541	0.006
H_3	3.856	0.074
H_4	3.478	−0.015
H_5	3.748	0.155
H_6	3.769	0.101
Rhodamine B		
H_{CH3}	1.115	−0.059
H_{CH2}	3.455	−0.079
H_A	6.624	−0.028
H_{B1}	6.772	−0.019
H_{B2}	6.786	−0.018
H_C	7.100	−0.013
H_D	7.313	0.068
H_E	7.608	−0.013
H_F	7.608	−0.013
H_G	7.834	−0.008

the larger shifts. These results prove unambiguously the inclusion of the RhB in the CD, which involves the ethyl amino groups [23].

^{1}H ROESY experiments can provide more detailed information about the inclusion mode through the intensity of the cross peaks in the 2D spectrum, related to the closeness between protons of host and guest. Fig. 4 shows expanded views of the correlation between the methyl group and aromatic protons Ha and Hb of RhB with the CD.

Strong ROE cross peaks arise between the H_3 and H_5 of the CD (3.76 ppm and 3.55 ppm) with the CH_3 group of the RhB, that of H_5 being the most intense. In addition, a small peak arises between H_6 and CH_3 protons. These interactions imply unambiguously that RhB is entering the cavity by the secondary hydroxyl rim. At 6.62 ppm and 6.78 ppm two more interactions arise, corresponding to the Ha and Hb from the RhB xanthene rings with the H_5 of the βCD. The intramolecular interaction of Ha and Hb with the CH_2− can be ruled out, as no cross peaks arise in the ROESY spectrum for the RhB alone in water, confirming the intermolecular interaction with H_5.

The fact that the interaction is taking place not in the central carboxyphenyl ring, but in one of the diaminoethyl groups opens the possibility of 2:1 complex, i.e. two CDs per guest. Job's continuous variation analysis [24] has been used to determine the actual stoichiometry. For this purpose samples at different molar ratios prepared with βCD and RhB concentrations ranging from 0 to 5×10^{-4} M were prepared in D_2O and analyzed by ^{1}H NMR spectroscopy.

The Job plot for protons H_3, H_2 of βCD and CH_3, H_G and H_D of RhB is shown in Fig. 5, so a signal from inside the βCD cavity and one from outside can be seen. The maximum change in the chemical shift takes place when the molar ratio is 0.5, inferring that the stoichiometry of the complex is 1:1.

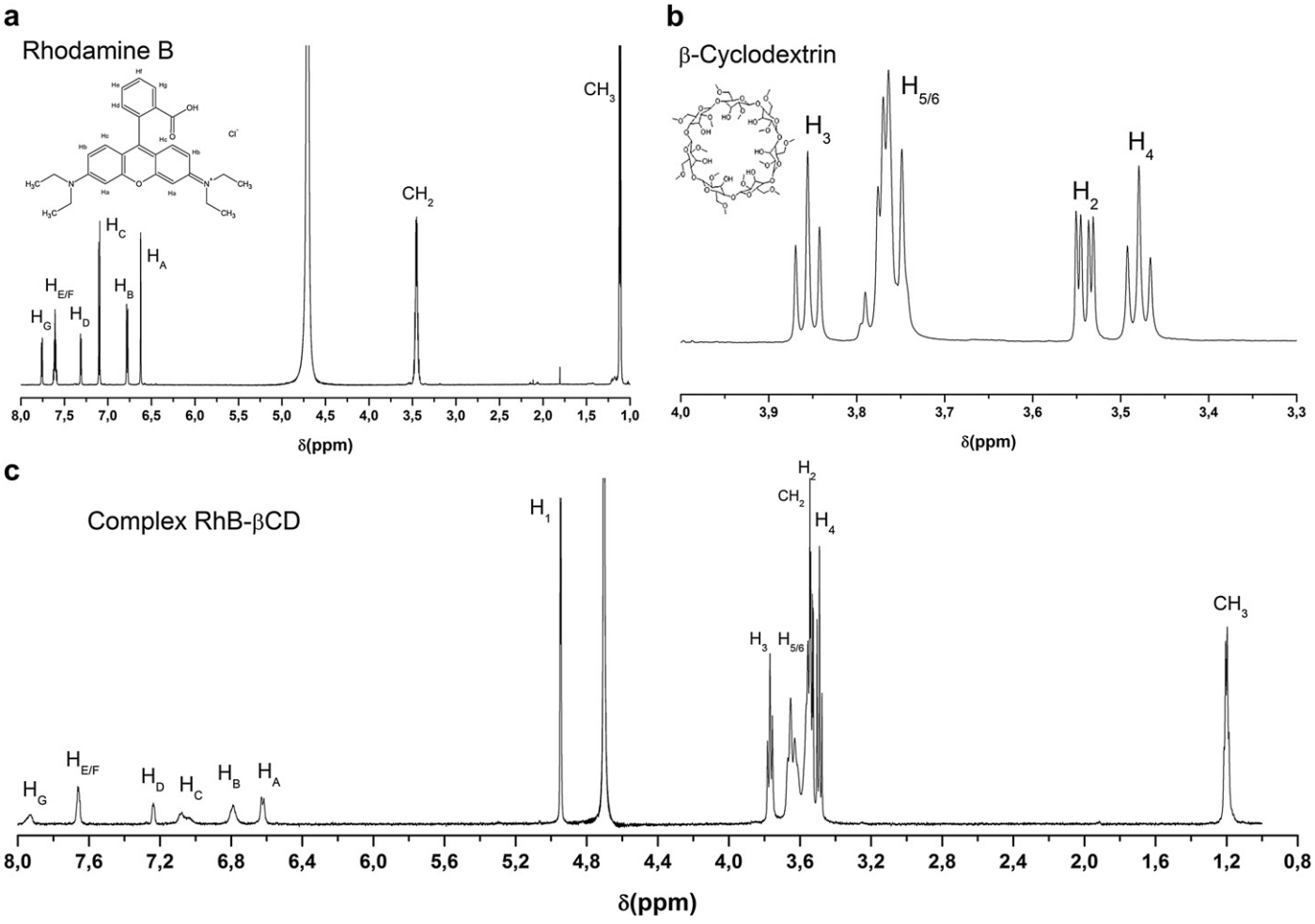

Fig. 2. ^{1}H NMR spectra in D_2O of: (a) RhB; (b) βCD; (c) molar ratio 1:1.

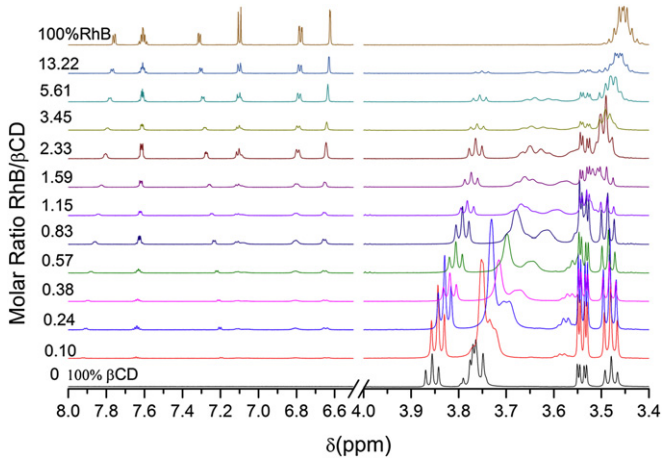

Fig. 3. ^{1}H NMR spectra of different molar ratios RhB:βCD. Concentrations of βCD and RhB range from 0 to 5 × 10^{-4} M.

As seen in Table 2, the protons of the carboxyphenyl ring also shift, although no NOE signals are detected. A possible explanation to the fact the stoichiometry sticks to 1:1 when having two diaminoethyl groups in the molecule, is that when the βCD approaches one of the diaminoethyl branches, it might induce the movement of the carboxyphenyl ring to the opposite side, as seen by the shift in

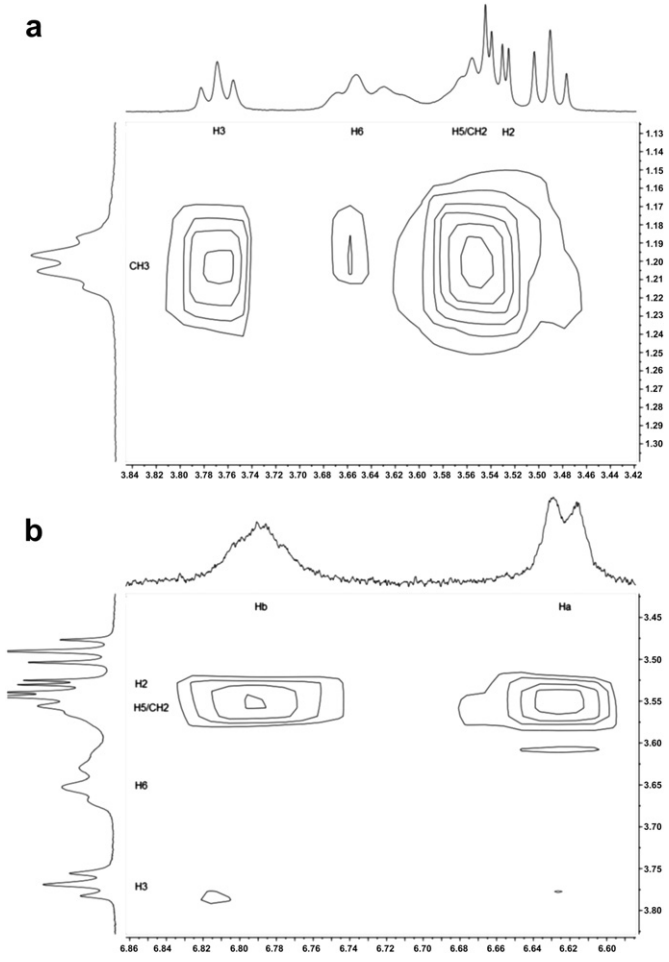

Fig. 4. (a and b). Zoomed view of the ROESY spectrum of RhB:βCD (1:1).

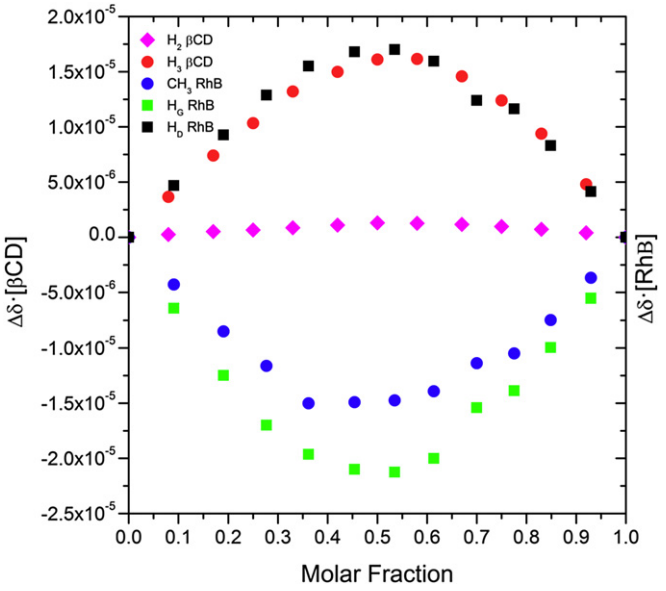

Fig. 5. Job plot for selected protons of βCD and RhB.

H_D, and thus the molecule is not receptive to dock with another βCD molecule in the other ring because of steric effects. Those same experiments were performed on the Rh6G–βCD system, but neither significant changes in the chemical shifts nor cross peaks in the ROESY spectrum were detected. These results confirm that only RhB forms a suitable stable inclusion complex with a 1:1 stoichiometry, where the βCD enters the RhB by one of its diethylamine sides.

Fluorescence emission can be used to gather precise information about the stability of the association. RhB presents a high fluorescence quantum yield, but it easily aggregates forming dimers and other species, especially in aqueous solution [25]. This process manifests as a quenching in the emission attributed to the long range dipole–dipole energy transfer from the monomer excited state to the aggregates [16] and also in bathochromic shifts from 587 nm to 650 nm in 10^{-3} M RhB solutions. Rhodamines and βCD may interact in different ways depending on the fluorophore concentration and its aggregation state. Thus, in dilute solutions of RhB, the βCD causes a decrease in emission due to the formation of the complex, less fluorescent than the free RhB. However, in conditions at which RhB is in the form of aggregates and its fluorescence quenched, the addition of βCD produces the opposite effect, yielding a fluorescent enhancement [26]. On the other hand, Rh6G does not aggregate as easily as the RhB [27] because of the bulkiness of the ester group in the phenyl ring and the methyl and ethyl substituents, which hinder the molecule stacking. Consequently, the presence of βCD enhances the emission in the case of Rh6G in aqueous solution.

The effect of successive additions of βCD to RhB 8 × 10^{-6} M is shown in Fig. 6. Free RhB has its maximum fluorescent emission at 582 nm, and experiences a slight blue shift of ca. 4 nm when βCD is added, along with a quenching in its fluorescence. Under our instrumental conditions, the linear response of the

Table 2
Binding constants for the complex βCD:RhB ([RhB] = 8 × 10^{-6} M).

	15 °C	25 °C	35 °C	45 °C	Δ*H* (kJ mol^{-1})	Δ*S* (J mol^{-1} K^{-1})
K·10^{-3} L mol^{-1}	5.1 ± 0.5	4.8 ± 0.2	4.1 ± 0.2	3.1 ± 0.2	−15 ± 3	21 ± 10

fluorescence for the RhB ranges up to 8×10^{-6} M, free of aggregation effects.

As the complex stoichiometry for the βCD is 1:1, its formation constant at a certain temperature can be expressed by the action mass law as:

$$K = \frac{[R:CD]}{[R][CD]} \tag{1}$$

being *R* the free fluorophore, *CD* the free βCD and *R:CD* the complex. In the experiments, the concentration of *R* is kept constant, varying that of *CD*. By combining the action mass law with the concentration mass balance for host and guest we get for [*R*] the following quadratic equation:

$$[R]^2 + \left(CD_0 - R_0 + \frac{1}{K}\right)[R] - \frac{R_0}{K} = 0 \tag{2}$$

The measured fluorescence at a certain wavelength, F_λ, is the result of the contributions of the two fluorescent species, *R* and *R:CD*, so thus

$$F_\lambda = F_\lambda^R + F_\lambda^{R:CD} = a_\lambda[R] + b_\lambda[R:CD] \tag{3}$$

where a_λ and b_λ are constants related to the fluorescence quantum yield and molar absorptivity of each fluorescent species at the excitation wavelength, λ, and to experimental conditions (source intensity, slit width and path length of the cell).

Dividing the above expression by $F_0 = a_\lambda R_0$, i.e., the fluorescence in the absence of cyclodextrin, eq. (3) can be written as

$$\left(\frac{F}{F_0}\right)_\lambda = [R] + \phi\frac{[R:CD]}{R_0} \tag{4}$$

where $\phi = b_\lambda/a_\lambda$. The experimental data at a certain emission wavelength can thus be fitted by a non-linear least-squares procedure to the above equation, in which ϕ and *K* are left as adjustable parameters. It is possible to improve the fitting using a wider set of data by taking into account the emission measured at each wavelength, and not only to a λ_{max}. A multivariable analysis can be performed by imposing the condition that the binding constants are the same for each wavelength. The error function to be minimized becomes

$$E = \sum_\lambda \sum_i \left(\left(F_i/F_{0,\lambda}\right)^{cal} - \left(F_i/F_{0,\lambda}\right)^{meas}\right)^2 \tag{5}$$

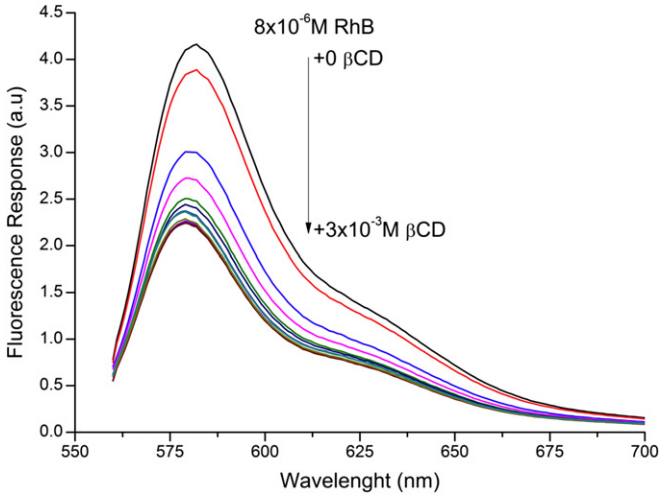

Fig. 6. Effect of the addition of βCD on the fluorescence of RhB 8×10^{-6} M in water.

where *i* sums over all the concentrations of CD and λ over all the wavelength range. The input parameter is a vector that contains the initial guess for the binding constants and ϕ_i, and the output is the estimation of the parameters with their error bounds, defined as the confidence intervals corresponding to a significance level, $\alpha = 0.16$. A weight factor, ω_λ, taken as the absolute value of the difference between $F_{0,\lambda}$, and the maximum value reached in the binding, is introduced at each wavelength in Eq (5), to give a higher statistical weight to that λ at which the changes in intensity are higher [28]. The enthalpy and the entropy have been obtained from the *K* dependence on the temperature through Van't Hoff equation and a weighted least-square method (Table 2).

The binding constants of RhB in water are relatively high, which indicates a stable association. The increasing temperature produces the diminution of *K*, as expected in an exothermic process. This same trend has been obtained by measuring at lower concentrations of RhB (data not shown). This stability with the temperature is important, considering that the formation of the nanocomposites requires conditions that, depending on the type of polymer, must be higher than 120 °C. As for the Rh6G:βCD system, it barely experiences changes in the emission by adding CD, resulting in the non-convergence of the fitting toward very low constants. This is a confirmation that there is no significant complex formation, in accordance with NMR data. It is worthy to mention that the enthalpy is not too high for these types of complexes, being the process controlled mainly by the entropy. According to ROESY data and considering the bulkiness of RhB and the size of the cavity, the

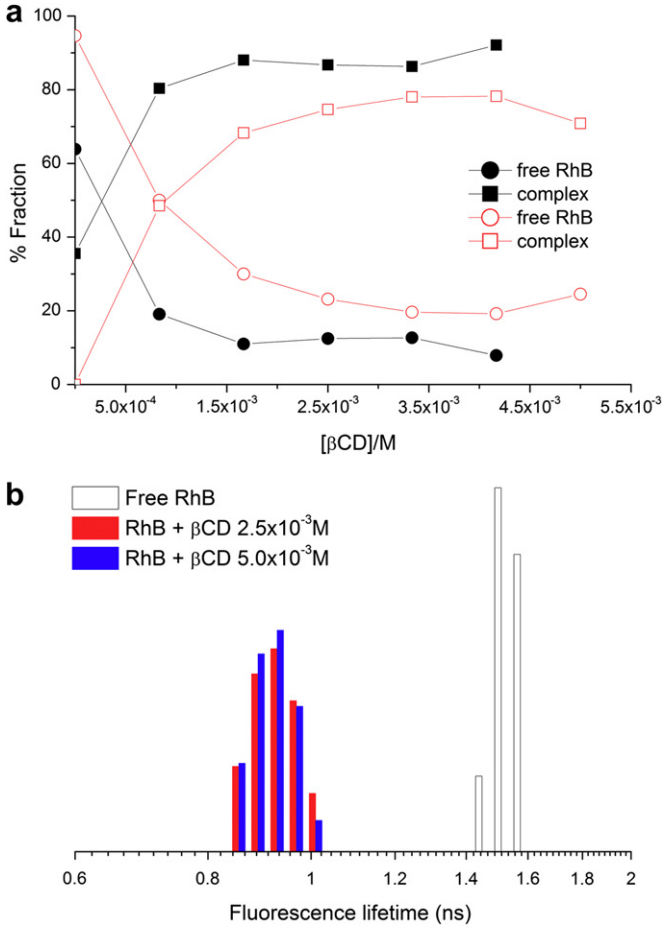

Fig. 7. Lifetime analysis: (a) fraction of the species found on 1×10^{-4} M (solid symbols) and 1×10^{-5} M (open symbols) of RhB upon addition of βCD; (b) Lifetime distributions.

inclusion is shallow and only part of the guest is included. Although the association constant is in good agreement with the one stated by Liu et al. [15], the enthalpy and entropy values are considerably different, as they obtain a non-expected positive $\Delta H = 40.8$ kJ mol^{-1} and $\Delta S = 0.21$ kJ mol^{-1} K^{-1} at 25 °C. These unusual values are reasoned in terms of the extra desolvation due to the lactonization of the hydrated benzoate moiety at the conditions of the experiment. It must be noticed that the constants obtained by this method are apparent constants, as the equilibrium between the cationic, lactone and zwitterionic form exists. However, as stated by Mchedlov-Petrossyan et al. [29] the fraction of the RhB molecules converting to the colorless lactone form in water at our concentration is less than 1%, so in our case we can rule out the lactonization effect mentioned before as being responsible for the different values. The use of a phosphate buffer 0.1 M to maintain the pH at 7.20 may be one of the reasons for this difference, as the ionic strength of the solution with this precise buffer is considerable and it is well known the quenching effect of some buffers on the fluorescence [30]. In our case, the pH has not been controlled by addition of buffers and the low concentration of RhB makes the ionic strength virtually zero.

In order to check the state of aggregation of the RhB at different concentrations and the effect the CD may have, fluorescence lifetime analyses were carried out upon these samples. In the experiments, RhB concentration was fixed at 1×10^{-4}, 1×10^{-5} and 1×10^{-6} M, and aliquots of a 5×10^{-3} M βCD stock solution were added to gradually increase the βCD concentration and induce the complex formation. The decay curves were processed by reconvolution distribution analysis at 200 intervals between 0 and 50 ns. Free RhB has a lifetime response of 1.7 ± 0.2 ns (Fig. 7), which correlates with the values found in the reference, 1.52 ns with emission at 400 nm and 1.68 ns at 560 nm [31]. Upon addition of βCD, a new mode appears with fluorescence lifetime of 0.75 ± 0.04 ns, which is retained upon successive additions (Fig. 7), its fraction increasing with the βCD concentration, accordingly to the shift of the equilibrium. When RhB 1×10^{-4} M is tested at 500 nm in the absence of βCD, a considerable fraction appears at approximately the same lifetime than the complex 0.97 ± 0.03 ns, which is attributable to the RhB aggregation effect at high concentrations. When RhB is at lower concentrations, from 1×10^{-5} to 1×10^{-7} M, and βCD is absent, this fraction does not appear and that corresponding to the free RhB is close to 100%. These results indicate the aggregation limit is between 10^{-4} M and 10^{-5} M for aqueous solutions, in good agreement with the literature values [32].

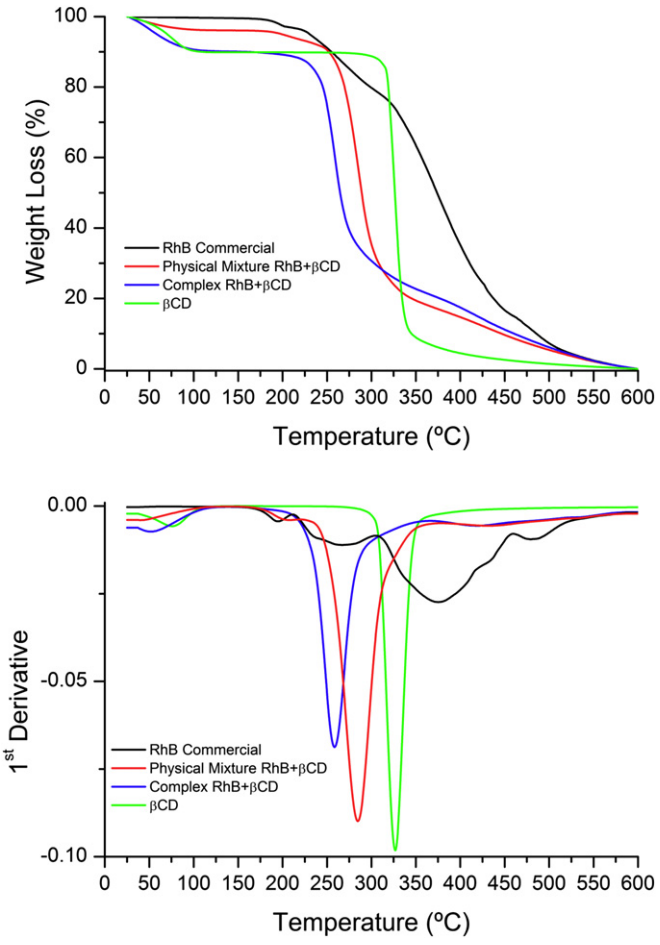

Fig. 8. TGA curves (top) and 1st derivative (bottom) of the RhB samples.

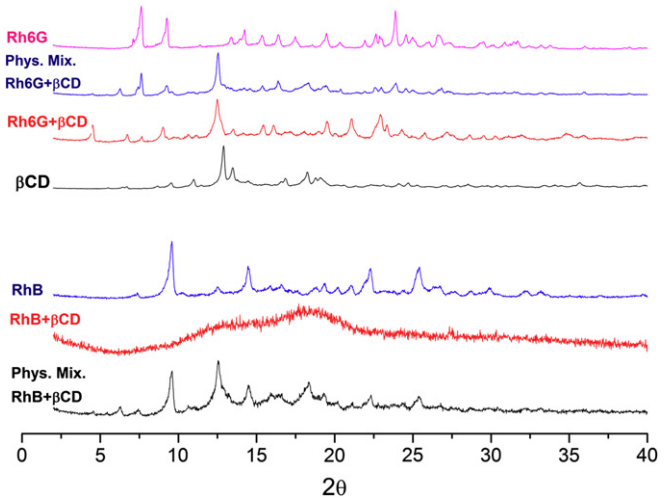

Fig. 9. X-ray diffractograms of the solid samples.

3.2. Solid complexes

The thermogravimetric analysis of the powder samples (Fig. 8) shows how the RhB presents at least a three-step decomposition

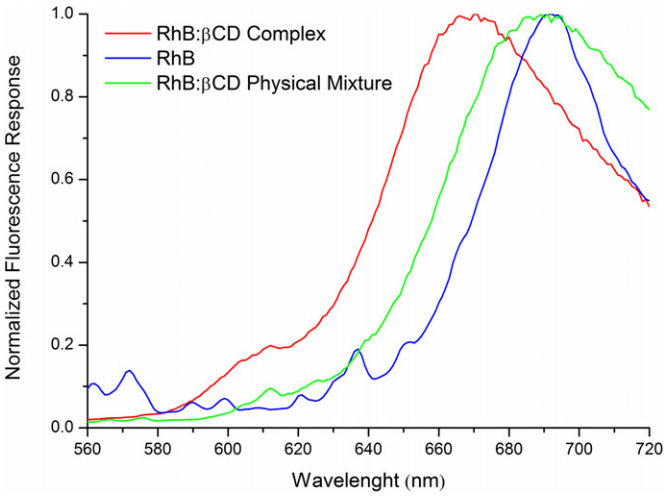

Fig. 10. Fluorescence response of the solid samples.

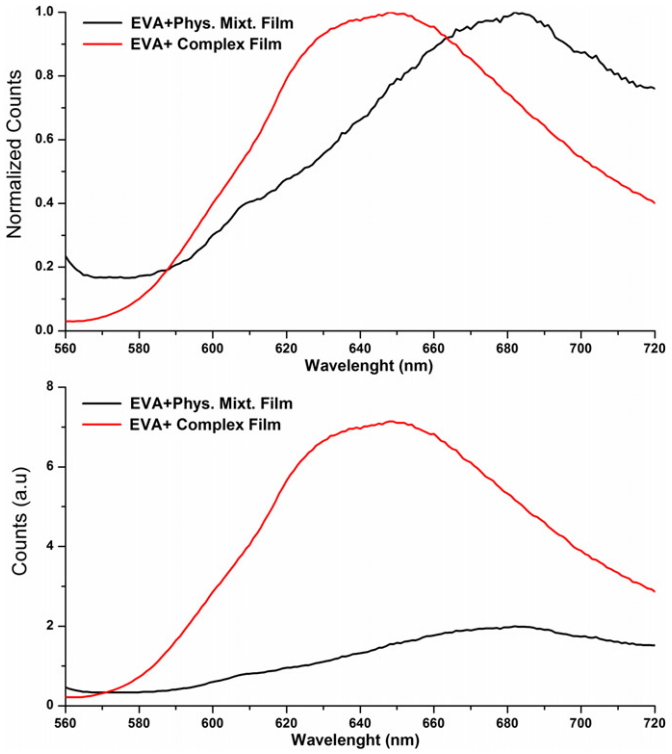

Fig. 11. Comparison of the fluorescence of films produced with RhB:βCD complex and the physical mixture. Top: normalized spectra; bottom: as measured.

process, starting around 180 °C and ending at 500 °C, and so does the physical mixture RhB-βCD. However, as confirmed by the first derivative trace, once the RhB:βCD complex is formed the decomposition process changes to a single step process, confirming that the inclusion yields a product with a different thermal behavior. This difference can be seen by the absence of the first minimum around 180 °C and the shift of the degradation temperature to 257 °C. When the same analysis is carried out with the Rh6G, only a slight shift in the temperature can be seen, but there is no evidence concerning the formation of a different product.

Confirming the results revealed above, FTIR-ATR analysis of the compounds shows that the RhB-βCD system presents important differences in the spectra compared to the physical mixture, whereas the Rh6B-βCD spectrum cannot be distinguished from the mixture. The strong band at 1587 cm^{-1} of RhB is assigned to the aromatic ring C–C vibrations and remains when forming the complex (data not shown). The rest of the RhB peaks in the aromatic region persist in the complex, while in the physical mixture they lose shape and are hidden in the baseline. Taking into account that the solid complex is formed from the aqueous solution, and with the previous data confirming that the Rh6G does not form complex with the βCD, we must conclude that the precipitate will be a bare physical mixture of both components.

X-Ray diffraction patterns (Fig. 9) corroborate the above results. The analysis shows a decrease in the crystallinity, as seen by the absence of peaks and the amorphous halo when the complex is formed in comparison to the commercial RhB and the physical mixture. The latter itself matches the sum of the RhB and the βCD diffractograms. As expected, Rh6G shows no evidence of complex formation.

Finally, solid state fluorescence measurements were also recorded on the commercial RhB, the physical mixture RhB-βCD and the RhB:βCD complex. The emission spectra show a 20 nm blue-shift upon complex formation. Commercial RhB has an emission peak at 690 nm, and the complex at 670 nm. The physical mixture behaves exactly like the commercial RhB (Fig. 10).

3.3. *Effect of milling*

The last step of the nanocomposite preparation is the milling of the fluorescent probe in its complex form with the polymeric matrix ensuring that the inclusion is kept after the HEBM and that the probe is homogeneously distributed throughout the matrix. It is known that the severe mechanical conditions occurring in these processes may break bonds or produce free radicals [9]. For this reason, the βCD has been milled alone under the same conditions as those of the films. According to ^1H NMR data, no changes are perceived in the spectrum after milling, which indicates that the process does not alter the chemical structure of the macrocycle. Regarding the nanocomposites, after the products were milled and processed into thin films, the fluorescence response of the film containing the RhB:βCD complex presented a four-fold fluorescence enhancement (Fig. 11, bottom) compared to the physical mixture and a blue shift of 40 nm (Fig. 11, top), which is in good agreement with the results of the solid samples before milling. It is worthy to mention that the trend is the same than in concentrated solution of RhB, where the fluorophore is extensively aggregated and the addition of βCD produces an enhancement on the fluorescent response, as explained above. All this confirms that the RhB:βCD complex can be used as a probe to monitor the dispersion of the oligosaccharide alone or attached to other nanostructure, as nanoparticles, as RhB behaves differently when bound to the βCD than when it is free in the matrix and that the complex is capable of enduring the extreme conditions of the HEBM process without losing its properties.

The films are shown in Fig. 12. The one containing the complex presents a uniform and homogeneous appearance in contrast to the

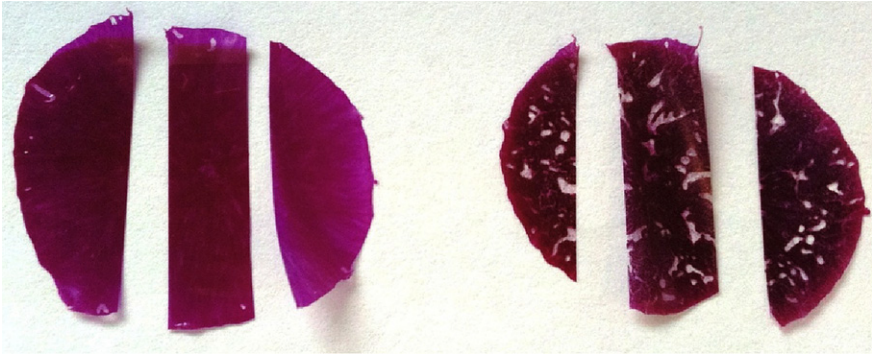

Fig. 12. Film formed with the complex (left) and with the physical mixture (right).

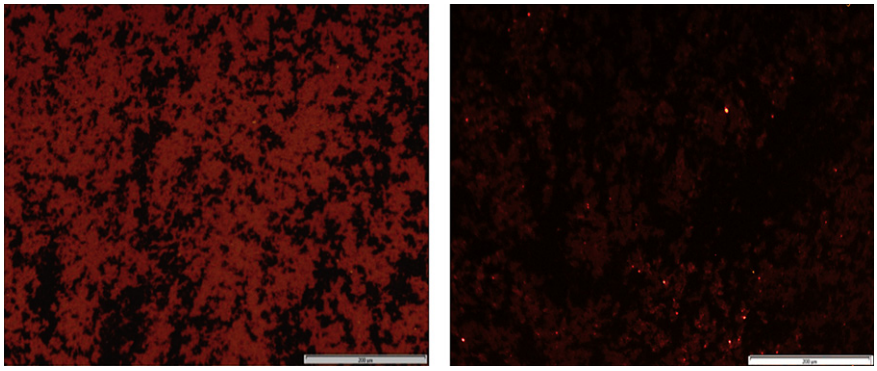

Fig. 13. 20× Fluorescent microscope image of the RhB:βCD complex film (left) and physical mixture (Right). Scale bar 200 μm. $\lambda_{ex} = 510$ nm.

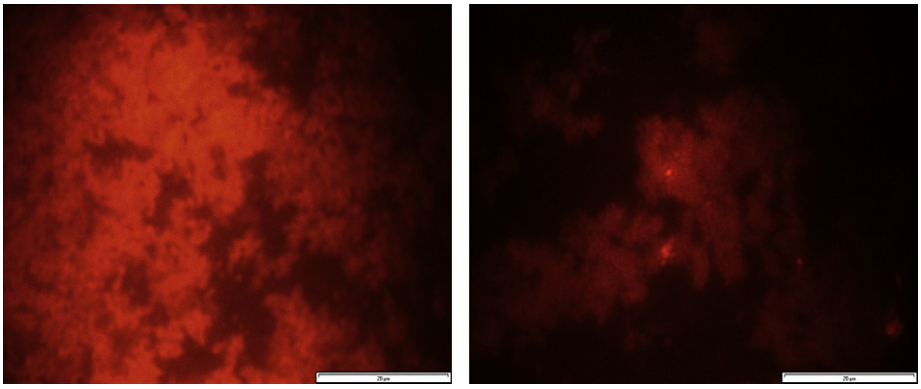

Fig. 14. 100× Microscope image of the RhB:βCD complex film (left) and physical mixture (Right). Scale bar 20 μm.

film with the simple physical mixture, also prepared by HEBM. The latter presents a darker color with white spots corresponding to macroscopic domains of aggregated βCD. As the complex lacks a crystalline structure, as XRD experiments have shown, it seems that in order to achieve a good dispersion of the βCD in the solid phase it is necessary to break its crystalline arrangement and convert it to an amorphous form.

Images at different scales of the films with the RhB:βCD complex and the physical mixture were taken with a fluorescence microscope. As it can be seen in Figs. 13 and 14, using the same diaphragm and magnification conditions (20× and 100×), the RhB:βCD film clearly shows an enhanced fluorescent response in relation to the other when excited at 510 nm. In addition to that, the complex produces an excellent dispersion throughout the matrix, whereas the mixture presents local domains of RhB at the bottom section and other sectors that are richer in βCD, where there is no fluorescence response at all resulting in a dark image.

4. Conclusions

The association between βCD and RhB and Rh6G has been studied both in solution and solid state by different techniques. ^{1}H NMR results combined with fluorescence spectroscopy confirm the formation of a stable complex of RhB of 1:1 stoichiometry, with a binding constant of the order of 10^4 M^{-1} on a wide range of temperatures. The mode of inclusion has been elucidated with the aid of ROESY spectra, proving that the RhB enters the βCD by any of the ethylammonium substituents toward the wider rim of the macrocycle, leaving exposed to the solvent the moiety of the RhB that bears the carboxylic group. Analysis of the solid products makes clear that the complex of RhB retains its stability in the solid phase, as stated by the disappearance of the endothermic peak at 200 °C in TGA, characteristic of the RhB, and to the blue shift and emission enhancement observed by fluorescence. On the other hand, Rh6G does not form complexes either in aqueous solution or in the solid phase.

The RhB complex mixed by cryo HEBM with the polymer, EVA, after the subsequent film production is homogeneously scattered through the matrix, undergoing a four-fold enhancement in its fluorescence, that is not observed with the physical mixture. The use of a fluorescent complex with βCD has thus the double effect of breaking the crystalline structure of the βCD by forming an amorphous phase that makes possible the proper dispersion of the macrocycle and to enhance the “visibility” of the macrocycle. These results, apart from eliminating the need of using more sophisticated techniques as SEM or AFM, are important for subsequent investigations of nanocomposites based in CDs, either as nanofillers by themselves or attached to other nanostructures.

Acknowledgments

Authors acknowledge the financial support of the projects MAT2010-16815 and CTQ2010-18564 from the Ministerio de Ciencia e Innovación, as well as the PhD grant for Rafael Serra provided by the “Asociación de Amigos de la Universidad de Navarra”.

References

[1] Hussain F, Hojjati M, Okamoto M, Russell E. Review article: polymer-matrix nanocomposites, processing, manufacturing and application: an overview. J Comp Mat 2006;40:1511–75.

[2] Zhao R, Torley P, Halley PJ. Emerging biodegradable materials: starch- and protein-based bio-nanocomposites. J Mater Sci 2008;43:3058–71.
[3] Suryanarayana C. Mechanical alloying and milling. Prog Mater Sci 2001; 46(1–2):1–184.
[4] Padella F, Incocciati E, Nannetti CA, Colella C, Casadio S, Magini M. Mechanically activated low temperature synthesis of Sr doped lanthanum manganite. Mechanically alloyed. J Metastable Nanocryst Mater Part 1 1998;269(2): 105–10.
[5] Rowlands SA, Hall AK, McCormick PG, Street R, Hart RJ, Ebell GF, et al. Destruction of toxic materials. Nature 1994;367(6460):223.
[6] Castrillo PD, Olmos D, Amador DR, González-Benito J. Real dispersion of isolated fumed silica nanoparticles in highly filled PMMA prepared by high energy ball milling. J Colloid Interface Sci 2007;308(2):318–24.
[7] Olmos D, Dominguez C, Castrillo PD, González-Benito J. Crystallization and final morphology of HDPE: effect of the high energy ball milling and the presence of TiO_2 nanoparticles. Polymer 2009;50(7):1732–42.
[8] González-Benito J, González-Gaitano G. Interfacial conformations and molecular structure of PMMA in PMMA/silica nanocomposites. Effect of high-energy ball milling. Macromolecules 2008;41(13):4777–85.
[9] Shaw WJD. Current understanding of mechanically alloyed polymers. Mater Sci Forum 1998;269(2):19–29.
[10] Padella F, Magini M, Incocciati EU. Patent N 0963825 B1, Bulletin; 2003/ 3956, 57.
[11] González-Gaitano G, González-Benito J. Pseudorotaxanes of cyclodextrin and diglycidyl ether of bisphenol A as precursors of new intramolecularly reinforced epoxy-based thermosets. Supramol Chem 2008;20:335–44.
[12] Xu M, Wu S, Zeng F, Yu C. Cyclodextrin supramolecular complex as a water-soluble ratiometric sensor for ferric ion sensing. Langmuir 2010;26(6): 4529–34.
[13] Patel K, Angelos S, Dichtel WR, Coscun A, Yang YW, Zink JI, et al. Enzyme-responsive snap-top covered silica nanocontainers. J Amer Chem Soc 2008; 130:2382–3.
[14] Wu J, Gao C. Click chemistry approach to rhodamine B-capped polyrotaxanes and their unique fluorescent properties. Macromol Chem Phys 2009;210: 1697–708.
[15] Liu Y, Chen Y, Li B, Wada T, Inoue Y. Cooperative multipoint recognition of organic dyes by bis(β-cyclodextrins) with 2,2′-bipyridine-4,4′-dicarboxy tethers. Chem Eur J 2001;7:2528–35.
[16] Saenger WR, Jacob J, Gessler K, Steiner T, Hoffmann D, Sanbe H, et al. Structures of the common cyclodextrins and their larger analogues – beyond the doughnut. Chem Rev 1998;98(5):1787–802.
[17] O'Conell RM, Saito TT. Plastics for high-power laser applications – a review. Opt Eng 1983;22(4):393–9.
[18] Peterson OG, Snavely BB. Stimulated emission from flashlamp-excited organic dyes in polmethyl methacrylate. Appl Phys Lett 1968;12(7):238–40.
[19] Crini G. Kinetic and equilibrium studies on the removal of cationic dyes from aqueous solution by adsorption onto a cyclodextrin polymer. Dyes Pigm 2008; 77:415–26.
[20] López Arbeloa F, López Arbeloa T, López Arbeloa I, Costela A, Garcia-Moreno I, Figuera JM, et al. Relations between photophysical and lasing properties of rhodamines in solid polymeric matrices. Appl Phys B 1997;64:651–7.
[21] Hwang TL, Shaka AJ. Water suppression that works. Excitation sculpting using arbitrary wave-forms and pulsed-field gradients. J Magn Reson Ser A 1995; 112(2):275–9.
[22] Bax A, Davis DG. Practical aspects of two-dimensional transverse NOE spectroscopy. J Magn Reson Ser A 1985;63(1):207–13.
[23] Bernini A, Spiga O, Ciutti A, Scarselli M, Bottoni G, Mascagni P, et al. Studies of the inclusion complex between β-cyclodextrin and paroxetine. Eur J Phar Sci 2004;22:445–50.
[24] Job P. Formation and stability of inorganic complexes in solution. Annali Chim Appl 1928;9:113–203.
[25] Mchedlov-Petrosyan NO, Kholin YV. Aggregation of rhodamine B in water. Russ J Appl Chem 2004;77(3):414–22.
[26] Degani Y, Willner I. Lasing of rhodamine B in aqueous solution containing β-cyclodextrin. Chem Phys Lett 1984;104(5):496–9.
[27] Politzer IR, Crago KT, Hampton T, Joseph J. Effect of β-cyclodextrin on the fluorescence, absorption and lasing of rhodamine 6g, rhodamine b and fluorescein disodium salt in aqueous solutions. Chem Phys Lett 1989;159(2–3):258–62.
[28] Sainz-Rozas PR, Isasi JR, González-Gaitano G. Spectral and photophysical properties of 2-dibenzofuranol and its inclusion complexes with cyclodextrins. J Photoch Photobio A Chem 2005;173:319–27.
[29] Mchedlov-Petrossyan NO, Kakhtik VI, Bezugliy VD. Dissociation, tautomerism and electroreduction of xanthene and sulfonephthalein dyes in N,N-dimethylformamide and other solvents. J Phys Org Chem 2003;16:380–97.
[30] Schulman SG. Acid–base chemistry of excited singlet states. In: Wehry EL, editor. Modern fluorescence spectroscopy, vol. 2. London: Heyden and Sons Ltd.; 1976. p. 239–74.
[31] Magde D, Rojas GE, Seybold P. Solvent dependence of the fluorescence lifetimes of xanthene dyes. Photochem Photobiol 1999;70:737–44.
[32] Ferreira JAB, Costa SMB. Non-radiative decay in rhodamines: role of 1:1 and 1:2 molecular complexation with β-ciclodextrin. J Photoch Photobio A Chem 2005;173:309–18.